2020 IEEE/RSJ International Conference on Intelligent Robots and Systems (IROS)
October 25-29, 2020, Las Vegas, NV, USA (Virtual)

FireAnt3D: a 3D self-climbing robot towards non-latticed robotic self-assembly

Petras Swissler and Michael Rubenstein

Abstract— **Robotic self-assembly allows robots to join to form useful, on-demand structures. Unfortunately, the methods employed by most self-assembling robotic swarms compromise this promise of adaptability through their use of fixed docking locations, which impair a swarm's ability to handle imperfections in the structural lattice resulting from load deflection or imperfect robot manufacture; these concerns worsen as swarm size increases. Inspired by the amorphous structures built by cells and social insects, FireAnt3D uses a novel docking mechanism, the 3D continuous dock, to attach to like robots regardless of alignment. FireAnt3D demonstrates the use of the 3D continuous docks, as well as how a robot can use such docks to connect to like robots and locomote over arbitrary 3D arrangements of its peers. The research outlined in this paper presents a profoundly different approach to docking and locomotion during self-assembly and addresses longstanding challenges in the field of robotic self-assembly.**

I. Introduction

Self-assembly is a technique by which many agents join to form larger structures, allowing swarms to adapt to their environment and carry out feats no individual agent could on their own. In nature, some examples of self-assembly include the ability of swarms of ants to build bridges [1] and towers [2], bees to form clusters [3] and festoons [4], and cells to form multi-cellular organisms. Such adaptability would be helpful for robotic applications in poorly-understood and dynamic environments, such as disaster relief, exploration, and construction, thus motivating research into robotic self-assembling systems.

One key difference between biological and robotic self-assembly is the organization of the structures formed. In biological self-assembling systems, the end-structures are typically amorphic (i.e. not constrained to a lattice), with insects grabbing each other at seemingly-arbitrary locations using their pincers and legs [5] [6], and cells attaching with any of the millions of proteins on their surface [7]. In contrast, most robotic self-assembled structures are constrained to lattices [8] [9] [10]. A fundamental reason for the use of latticed structures is the use of discrete attachment locations by most modular [11] and structure-building robots [12]. This results in a need for specific alignment between attachment mechanisms via passive hardware [10] [12] [13], requiring the use of sensors for active alignment [14] [15], or relying on module deformation [16]. Such systems must align their attachment faces within some tolerance [17] [18] since misalignment could defeat attachment attempts [19].

Authors are with the Department of Mechanical Engineering, Northwestern University, Evanston, IL, USA. e-mail: petrasswissler2022@u.northwestern.edu, rubenstein@northwestern.edu

Fig. 1: FireAnt3D climbs atop a collection of its peers by flipping about strong connections it made using its 3D continuous docks. The robot attaches to like robots without alignment, allowing for simple locomotion.

This reliance on specific attachment locations is particularly problematic in the context of large-scale self-assembly: the need for low-cost robots compels the use of loose manufacturing tolerances [16] [20]. Therefore, large-scale self-assembled robotic structures are particularly vulnerable to having misalignment between attachment surfaces due to tolerance stack [21]. Such large-scale structures are also likely to experience localized or global deflection due to gravitational or other loads during assembly, again leading to misalignment between attachment surfaces. The resulting invalid or missed connections could weaken or prevent the completion of self-assembled structures.

The use of fixed attachment points also impacts robotic self-assembly algorithms: most algorithms seek to achieve a priori, latticed shapes [12] [22] [23], and often exploit the known docking locations by using the relative positions of modules to gain perfect knowledge of a robot's location in the global shape [22] [23]. This contrasts with behaviors exhibited in biological self-assembly (which generally use free-form connections), where environment-adaptive self-assembly appears to result from agents reacting to local information [1] [3] rather than acting to form some prescribed shape. Recent work has shown that robots following bio-inspired behaviors were able to build unplanned, useful structures [24] [25].

Although several robots can form attachments without dock-to-dock alignment [25] [26] [27] [28], this capability has thus far been constrained to a 2D plane, and connections are often weak [26] [27]. Some of these implementations also

978-1-7281-6211-9/20/$31.00 ©2020 IEEE

require specific alignment of the attachment mechanism to its neighbors' body [25] [28].

Another major challenge in large-scale self-assembly is the addition of agents to the structure. One approach is to rely upon external forces to randomly bring agents into contact with the structure [9] [13], but this gives up the robots' ability to operate independently and in arbitrary environments. Another approach is to lay down and climb passive structural members [12] [24], but this introduces bottlenecks in the speed of assembly from the need to return to pick up more structural members, and the need to plan paths to avoid other workers [12]. Other platforms rely on neighboring agents to pass robots around the structure [8] [17] [29], but this requires large-scale cooperation amongst robots and could be interrupted by dead agents.

A locomotive approach that more closely matches the self-assembly of social insects is to have agents climb over their peers. Self-climbing allows agents to unilaterally decide when or if to continue motion along the structure, granting greater autonomy to the agents and allowing self-assembly without help from peers or specific environments. Such locomotion is difficult, however, with few robots having achieved unaided self-climbing [10] [25] [30] [31].

For robots using fixed attachment points, kinematics and motion planning of locomotion must be carefully considered to ensure that a moving robot reaches a fixed location with each step to ensure proper dock alignment [29] [32]. Without the need for alignment between robots, locomotive kinematics becomes much less important, although analysis of large-scale dynamics and kinematics of a self-assembled structure would be more complex.

To our knowledge, only the original FireAnt [30] has demonstrated the ability to form robust connections to its peers while self-climbing, something critical for the self-assembly of strong structures, and it does so without the need for fixed attachment points. The original FireAnt, however, was a 2D robot and thus could only operate in limited environments. To enable FireAnt3D to operate in a 3D space, a wholly new design was required: the original FireAnt exploited its 2D nature by placing most components out-of-plane of its 2D continuous docks and by operating on an inclined surface to reduce the effective gravity. The robot also used an out-of-plane ground rail to provide a common ground between robots, something not possible in 3D. The move to 3D also made necessary a fundamental redesign of the continuous docks.

FireAnt3D is a robot that uses its 3D continuous docks to form strong, arbitrary, and non-latticed connections to its peers, and climbs its peers using a flipping locomotion. The robot was developed for three main purposes: first, to demonstrate the use of the 3D continuous docks; second, to demonstrate a robot capable of forming arbitrary, non-latticed 3D connections with like robots; third, to demonstrate how such a robot could locomote over arbitrary arrangements of its peers.

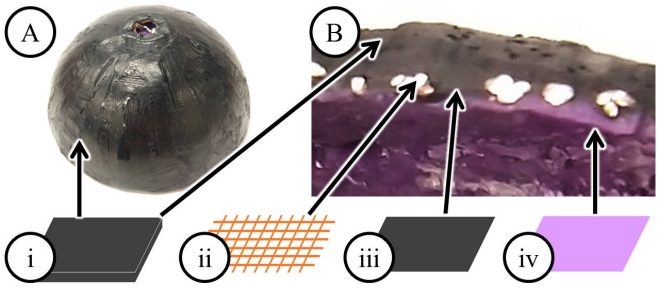

Fig. 2: The continuous dock (A) consists of four main layers. Shown in cross-section (B), these layers are, from outermost to innermost, (i) a 1.4 mm layer of conductive plastic, (ii) a sheet of 67% open copper mesh, (iii) a 0.2 mm layer of conductive plastic, and (iv) an insulating layer made of non-conductive plastic. A 3D printer prints these layers as 2D shapes, which are then assembled, heated, and pressed into a forming mold.

II. The 3D Continuous Dock

A. Design and principles of operation

The 3D continuous dock allows any two contacting docks to form strong attachments regardless of the position or orientation of contact. The docks attach and detach by melting together their outermost layers by joule-heating their conductive plastic. This allows two robots using such docks to form attachments without the need for alignment, assuming that the robot design is such that any approach by a like robot will only ever touch a docking surface, as is the case with FireAnt3D. This capability is similar to the continuous docks demonstrated on the original FireAnt [30], but with capabilities extended to form attachments with any 3D contact, rather than being limited to a plane. In the implementation shown in this paper the docks are hemispheres, but could take different forms for different applications.

Docks consist of the four layers shown in Fig. 2. The outer layer is the material that bonds with other docks and is sufficiently thick to account for the surface flattening that occurs during attachment, as well as to protect against any minimal material transfer that may occur when the docks detach. This outer layer is made of Proto-pasta conductive PLA and has a conductivity of 15 ohm-cm [33]. Below this is a copper mesh that is the primary electrical path for current flow during attachment. A second sheet of conductive plastic is below the copper mesh. During dock construction, these top three layers are heated under pressure to bond the two layers of conductive plastic through the holes in the mesh, thus ensuring uniform contact between the conductive plastic and the copper mesh and helping to prevent delamination. The presence of the copper mesh in the composite material strengthens the dock during attachment, since the mesh stiffens the dock against the softening of the plastic that occurs while heating. An inner insulating layer protects any components inside the dock.

The final major component of the 3D continuous dock system is the ground-return hoop. Illustrated in Fig. 3, when the robot starts an attachment or disconnection between two touching docks, it first applies a voltage to the dock relative to the ground-return hoop. The robot then sweeps

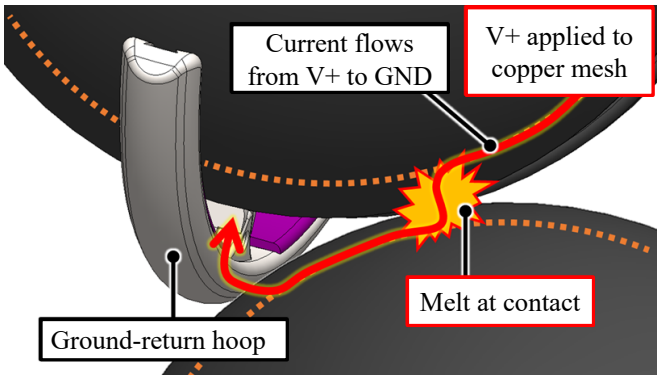

Fig. 3: Current flows from the attaching (top) dock to the passive dock (bottom), then back into the hoop of the attaching dock. In the case of attachment, this melts the docks together, forming a strong bond. Docks detach by repeating this process to melt and weaken the connection.

this hoop until both the docking surface and the ground-return hoop contact the dock to which the robot will attach. Current then flows primarily along the copper mesh until it must pass through the conductive plastic to reach the other dock, heating and melting the conductive plastic only at the location of contact. Current then flows primarily along the copper mesh of the other dock until it must once again pass through the conductive plastic to reach the ground-return hoop. The thermal mass of the hoop and the differing coefficients of thermal expansion minimize adhesion of the ground-return hoop to the second dock.

Two newly attached docks passively cool after melting together, forming a strong and rigid bond. To detach, voltage is re-applied to melt the docks and weaken the bond, making it easy to pull apart. Disconnection rarely results in the spike formations seen on the original FireAnt [30] and rarely results in unequal distribution of material between the two docks.

Based on developmental tests performed on a specialized test rig, a given attachment location on a dock surface has a lifespan of about 50 attachment / disconnection cycles before connections become unreliable, with failed connections becoming common after about 100 cycles. The part cost of a single dock hemisphere is approximately 8 USD, and it is possible to replace the docks on FireAnt3D by removing a single bolt and unplugging a wire. It is also possible to refurbish the docks throughout their lifetime to a like-new state by using a soldering iron to smooth existing plastic and melt new conductive plastic onto the dock.

B. Robot Attachment Parameters

Forming successful attachments with the continuous docks requires a balance of three primary parameters: voltage applied, time-integrated current passed, and press force. All discussion of attachment parameters in this section is in context of their use on the FireAnt3D robot.

FireAnt3D uses a nominal voltage between the attaching dock and its hoop of 33.3 V (9 lithium polymer battery cells). This relatively high voltage is necessary due to the high resistance of the initial interface between docks. Once melting begins, the interface area between docks increases, eventually reducing the resistance between docks to approximately 10 ohms.

The time-integrated current passed through the dock is the single most reliable predictor of attachment strength and is thus the metric used to determine when the attachment process is complete. The time-integrated current passed during attachment must be sufficient to adequately melt the conductive plastic at the attachment interface. However, it is desirable to use the minimum time-integrated current that will result in reliable connections, since battery life concerns prevent the use of arbitrarily high integrated currents for heating. Based on iterative testing, FireAnt3D passes 30 A-s during attachment.

Finally, some press force during attachment is necessary to ensure a strong connection. A need to balance press force and attachment strength arises because an attachment completed using some press force must allow the robot to exert that same force during a future attachment. It is also necessary to keep the press force below the capability of the drivetrain. Based on iterative testing of robot locomotion, a nominal per-dock press force of 4.9 N (1.1 lbf) is used for locomotion on a floor of other robots.

C. Demonstration of Dock Strength

An experiment was performed to quantify the tensile strength of dock connections. Three docks arranged in an equilateral triangle were mounted on a wood board, as shown in Fig. 4. This arrangement provided a consistent and easily repeatable attachment configuration that mitigated the presence of bending moments as the docks were pulled apart. A 14.7 N (3.3 lbf) (4.9 N (1.1 lbf) per connection) press force was applied as the three docks were simultaneously attached to a single dock by applying a 33.3 V load to the single dock and simultaneously passing a total of 30 A-s through the each of the three connections. The connections then cooled for a minimum of 5 minutes. The bonded docks were mounted on a linear test stand and a linear actuator smoothly increased the pull force until all attachments broke, with a scale measuring the pull force.

Across ten trials, the average break force for the dock arrangement was 767 N (172 lbf), with a maximum break force of 1036 N (233 lbf) and a minimum break force of 540 N (121 lbf). These results are a conservative estimate of the tensile strength of the dock attachments since the attachment faces between the docks were approximately 30 degrees from horizontal, meaning that the load had a significant shear

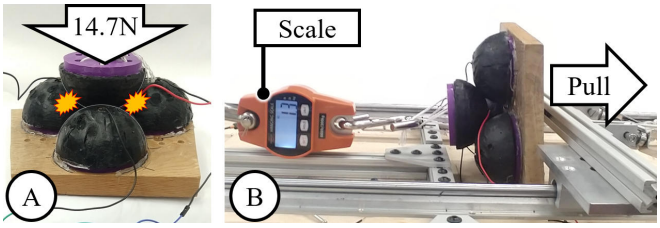

Fig. 4: (A) A load is applied to a single dock as a microcontroller controls its attachment to an arrangement of three other docks. (B) A linear actuator pulls the docks apart until all connections fail.

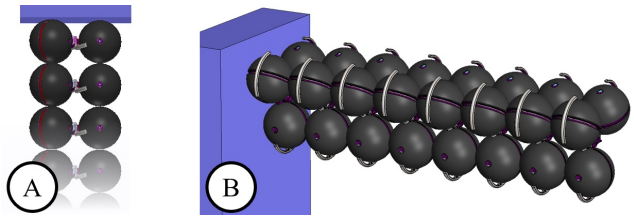

Fig. 5: The strength of the 3D continuous docks will enable future swarms to build (A) long chains and (B) cantilever structures.

component (materials are generally weaker in shear than they are in tension).

Assuming each connection experienced the same load, the average break force of a single connection was 23 times the 10.8 N (2.4 lbf) weight of the robot. Assuming the best-case structures shown in Fig. 5, this strength corresponds to a vertical chain of robots up to 71 dock diameters long, and a cantilever of robots up to 8 dock diameters long.

III. FireAnt3D Design

A. Mechanical Design

The mechanical design of FireAnt3D focused on two objectives. First, the design must enable FireAnt3D to locomote over arbitrary arrangements of its peers. Second, any approach by a like robot should only ever contact a dock. Fig. 6 shows the resulting design, which fits in a spherical envelope of diameter 212 mm (8.35 in).

FireAnt3D consists of three identical, 85 mm (3.4 in) diameter, semi-autonomous spheres joined at a centerbody. A bearing at the interface between the sphere arm and the centerbody allows the sphere to pivot passively in the socket. The centerbody flexes slightly when a sphere exerts a press or pull load using its arm, allowing two force sensing resistors to measure this force.

Each sphere has two locomotive degrees of freedom. The spheres can move their arm (lifting or lowering the centerbody and other docks) and passively pivot within their socket in the centerbody. The spheres also have two degrees of freedom associated with attachment formation: hoop position and dock voltage. Hoop motion and arm motion are relative to the dock and are independent from each other. A sphere can also push its hoop against the centerbody to restrict passive rotation in the centerbody.

The sphere arm divides the spheres into two halves. As seen in Fig. 7, one half of the sphere simply holds the battery, while the other half holds the drive system and electronics. Each sphere drives its actuated degrees of freedom using two 6 V N20 electric motors. One motor drives the hoop using a drivetrain with a 1154.75:1 gear reduction. The other motor drives the arm using a drivetrain with a 31840:1 gear reduction; the arm drivetrain incorporates a worm gear to prevent back-drive, allowing the arm to maintain some applied force without stalling the motor. When the robot drives its arm, wiring to the centerbody coils and uncoils within a cavity in the center of the sphere. Because of this design, the arm only rotates 315 degrees relative to the docks, sufficient for FireAnt3D to locomote on like robots.

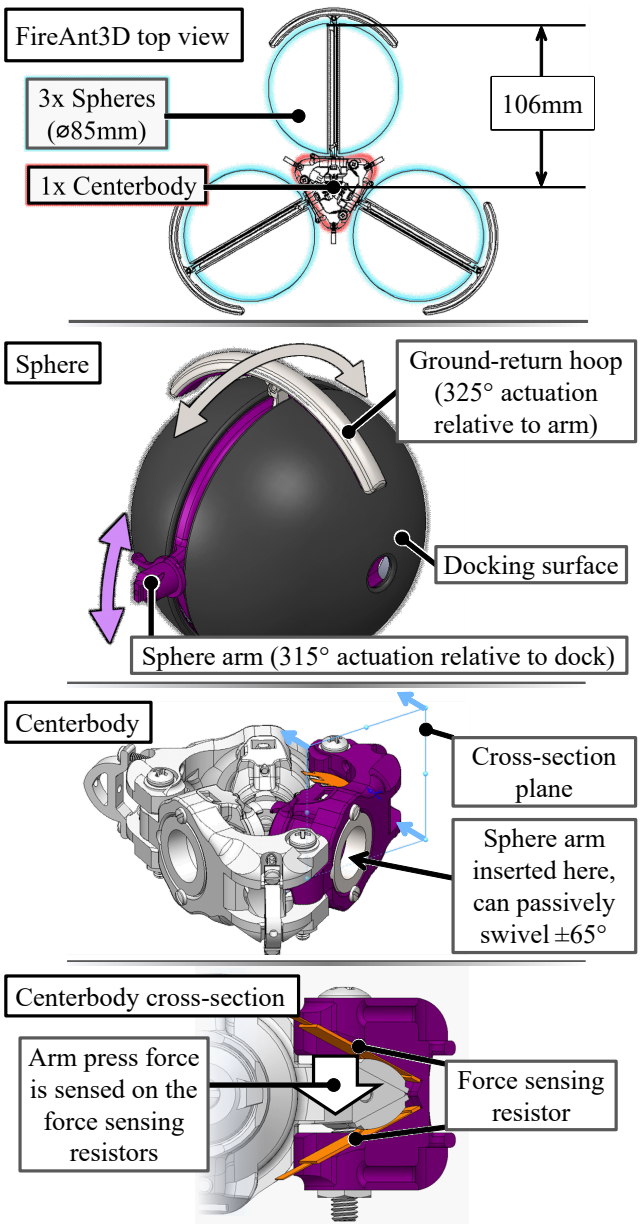

Fig. 6: FireAnt3D is rotationally symmetric, with a centerbody joining three identical spheres, each of which is covered in a 3D continuous dock.

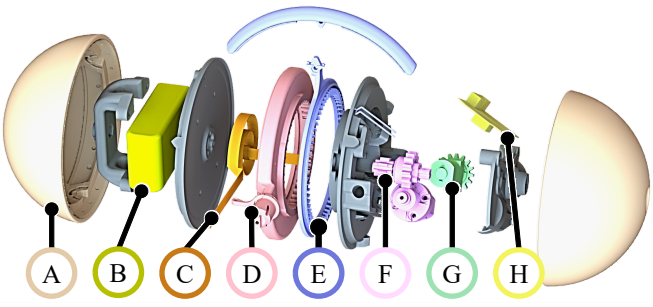

Fig. 7: Each sphere contains: (A) continuous dock shells; (B) a 3S, 450 mAh LiPo battery; (C) a coiled ribbon cable that electrically connects the sphere to the centerbody; (D) a press arm that is inserted into the centerbody and allows the sphere to exert a force on the centerbody; (E) a ground-return hoop; (F) a motor and drive system for moving the press arm; (G) a motor and drive system for moving the ground-return hoop; (H) control electronics.

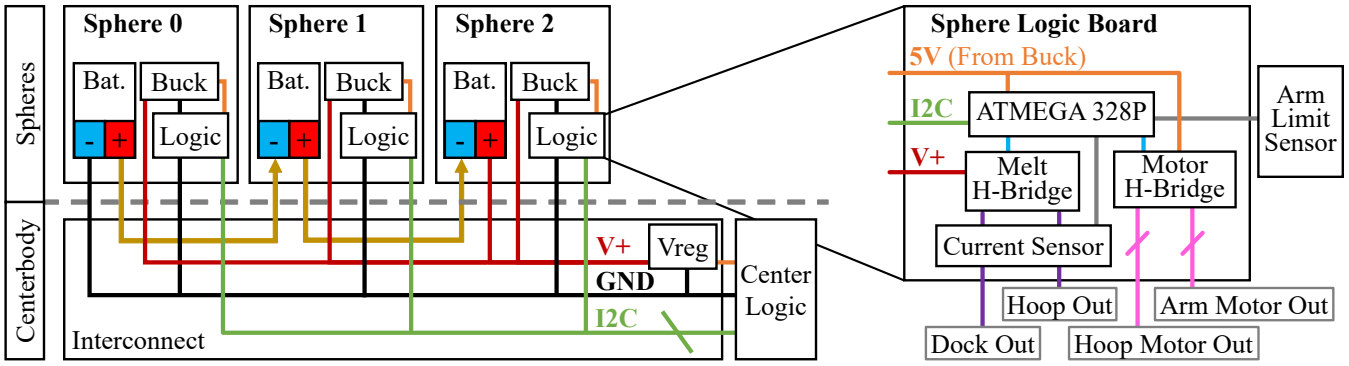

Fig. 8: Wiring from each sphere is joined at the centerbody, distributing power and allowing the centerbody logic board to command each sphere.

B. Electrical and Logical Design

Fig. 8 shows an overview of the electrical design of FireAnt3D. Each sphere holds an identical set of circuit boards, electrically joined in the centerbody of the robot. The centerbody has two circuit boards. The first is a logic board with an ATmega328PB microcontroller and hardware for force sensing. The microcontroller sends instructions to the spheres via I2C and receives high-level commands from human operators via a serial communication line. The second centerbody circuit board is a simple interconnect board for the six wires going to each sphere: a common ground, negative battery voltage, positive battery voltage, a V+ high voltage line, and the SCL and SDA lines for I2C communication. The interconnect board chains the sphere batteries in series to supply a single nominal V+ voltage of 33.3 V to the entire robot.

Each sphere also holds two circuit boards. The first is a buck converter that efficiently converts V+ to 5 V. The second board is the sphere logic board with an ATmega328P microcontroller that receives I2C instructions from the centerbody logic board and implements the requisite low-level behaviors using two sensory inputs and three outputs.

The two sensory inputs are dock current and the arm rotation limit. The microcontroller senses current using shunt current monitors that measure both small currents (to detect the initial contact of the hoop to the attaching dock) and large currents (to measure and monitor attachment and disconnection currents). The arm limit sensor detects when the arm has reached its hard-stop rotation limits by shorting a digital input pin to ground.

The three sphere outputs are the arm motor, the hoop motor, and the dock state. A single H-bridge controls both motors using the 5 V output of the buck converter. A different, higher-power H-bridge controls the state of the ground-return hoop and dock, allowing both the hoop and dock surface to be independently tied to V+, GND, or float at a high-z state.

C. Locomotion

Robot locomotion follows the six phases shown in Fig. 9. All flipping motions use bang-bang control of the arm motors and are open-loop with the exception of ending the flip after meeting some desired press force.

In Fig. 9 the robot has just flipped about sphere A, and has just attached on sphere B. Locomotion proceeds as follows:

- *Detach*: FireAnt3D detaches the dock of sphere A by first having sphere A press down on spheres B and C (this increases the reliability of disconnections). The robot then preloads a lifting force using sphere B. Sphere A then executes its detaching behavior by sweeping its ground-return hoop towards the attachment interface and melting the point of contact, weakening the bond and allowing disconnection to occur. The ground-return hoop also provides additional lifting force to aid disconnection.
- *Flip*: The robot flips forward about sphere B to lift spheres A and C clear of obstructions.
- *Prepare*: Spheres A and C execute a preparation procedure in which the hoops are brought forward and the spheres are rotated to allow them to perform the next locomotive step if selected as the next attaching sphere. This step is necessary because the spheres cannot continuously rotate.
- *Flip*: The robot continues rotating about sphere B. Either sphere A or C will eventually contact another sphere from a different robot.
- *Settle*: FireAnt3D continues flipping forward about sphere B, causing the centerbody to pivot about its passively-actuated degree of freedom, thus allowing the robot to settle such that both spheres A and C are pressed against their respective contacting spheres with some desired force.
- *Attach*: Sphere C is selected as the next attachment sphere and it sweeps its ground-return hoop towards the attachment point, allowing the docks to melt together. This connection then passively cools.

A single step takes approximately 6.5 minutes with the duration of each step varying based on how far the robot must flip. FireAnt3D spends about 1.5 minutes preparing, 1.5 minutes flipping forward, and 3 minutes cooling (a very conservative duration), with attaching and detaching taking about 15 seconds each. The speed of locomotion was not prioritized for FireAnt3D and could improve by using more powerful motors and a less conservative cooling duration.

One important benefit of this style of locomotion is that FireAnt3D can use the same locomotive procedure regardless

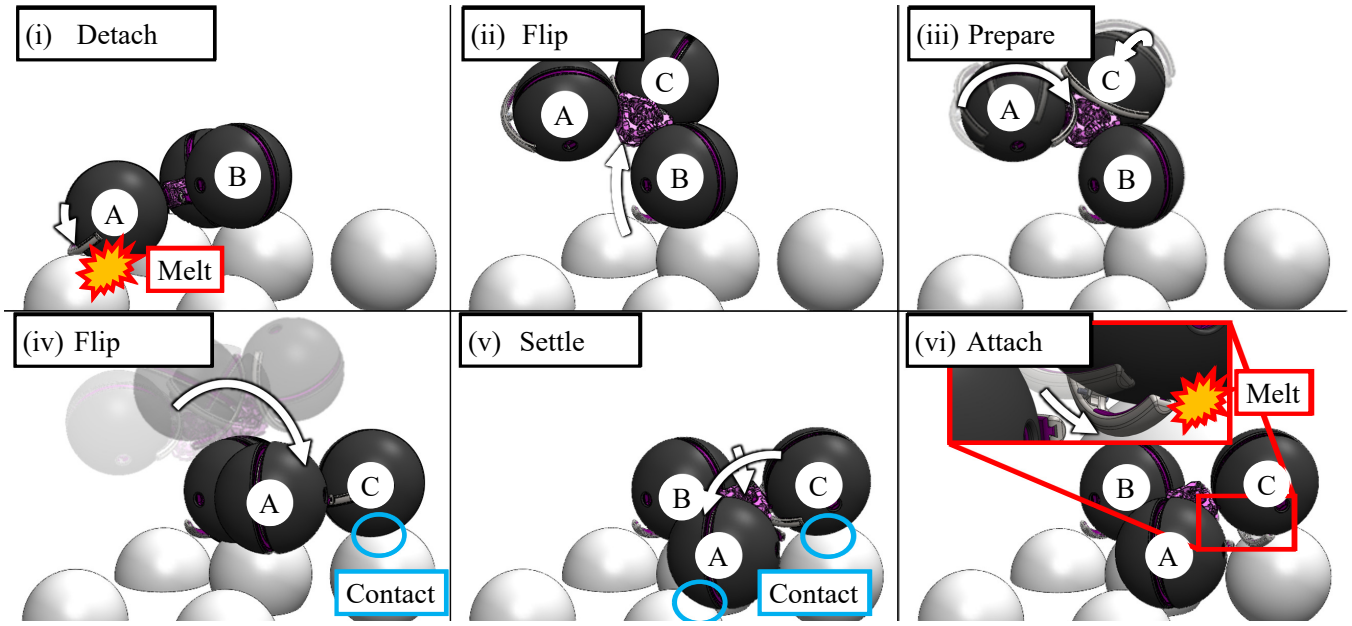

Fig. 9: FireAnt3D locomotion follows a simple sequence with minimal sensing and actuation requirements.

of the orientation of the surface on which it climbs, whether it be a floor, wall or ceiling. This ability to climb on all orientations is important in the context of robotic self-assembly, where it may be necessary to add to a structure in unpredictable locations. Constraints on the types of surfaces on which a robot can locomote would limit how a structure is built (limiting on-the-fly adaptability), or limit the types of structures that could be built.

This method of locomotion also minimizes sensing requirements. A single step only uses three sensors: a current sensor for the detaching dock, a current sensor for the attaching dock, and the force sensing resistors used to measure press force. A fully automated robot would require additional sensing to decide on the direction of the next step; FireAnt3D relies on remote control by a human operator.

FireAnt3D's locomotion also removes the need for precise kinematics or carefully-planned motion: a step only uses a single motor for forward motion, and continuous locomotion only uses a total of three motors (in addition to those driving the ground-return hoops during attachment and disconnection). The 3D continuous docks enable this locomotive simplicity because it removes the need for precise placement of the next step.

IV. Demonstration of Locomotive Ability

An experiment was performed to demonstrate FireAnt3D locomotion in a real-world environment on a floor, wall, and ceiling of its peers, as shown in Fig. 10. The test arena consists of four geometrical copies of FireAnt3D, mounted on an aluminum frame and arbitrarily arranged to simulate a self-assembled FireAnt3D structure. These copies use the same 3D continuous docks as FireAnt3D and are equivalent to real FireAnt3D robots with docks set to a high-Z state.

At the start of each test, a human operator pressed FireAnt3D into the arena surface as the robot attached itself to the arena. The robot then locomoted about the arena surface under its own power. An operator directed this locomotion by specifying the direction of each step, with the robot executing the step autonomously. FireAnt3D locomoted about the arena in three configurations: floor, wall, and ceiling. For the floor and wall configurations, FireAnt3D used a nominal press force of 9.8 N (2.2 lbf) and using 7.8 N (1.8 lbf) for the ceiling. Observations of locomotive reliability during preliminary testing drove this difference.

In testing the three configurations, FireAnt3D executed 9 consecutive steps over a floor made of its peers, 4 on a ceiling made of its peers, and 4 on a wall made of its peers; the final step was the one during which it failed.

This reliability is less than desired, a shortcoming primarily due to three specific, addressable deficiencies in the robot design. First, the plastic gears used in the sphere arm drivetrain were not strong enough to repeatedly apply the desired press force, resulting in damage to the gears; ceiling locomotion was particularly difficult in this respect because the robot needs to press at the same time as counteracting gravity. Second, if the centerbody pivoted too far, the axis of measured force and the axis of applied force would diverge too greatly, leading to the robot trying to press down with too great a force. This led to either drivetrain damage or too great a bending moment at the dock attachment, cleaving the connection. Finally, the force sensors had a high degree of hysteresis and were not independent of laterally-applied loads, limiting their reliability.

V. Conclusion

FireAnt3D successfully locomoted over its peers in all three arena orientations. This testing thus demonstrated FireAnt3D's use of its 3D continuous docks to form strong, arbitrary, and non-latticed connections to its peers, as well as the use of such connections to climb its peers, meeting all primary goals and demonstrating an all-new robot concept.

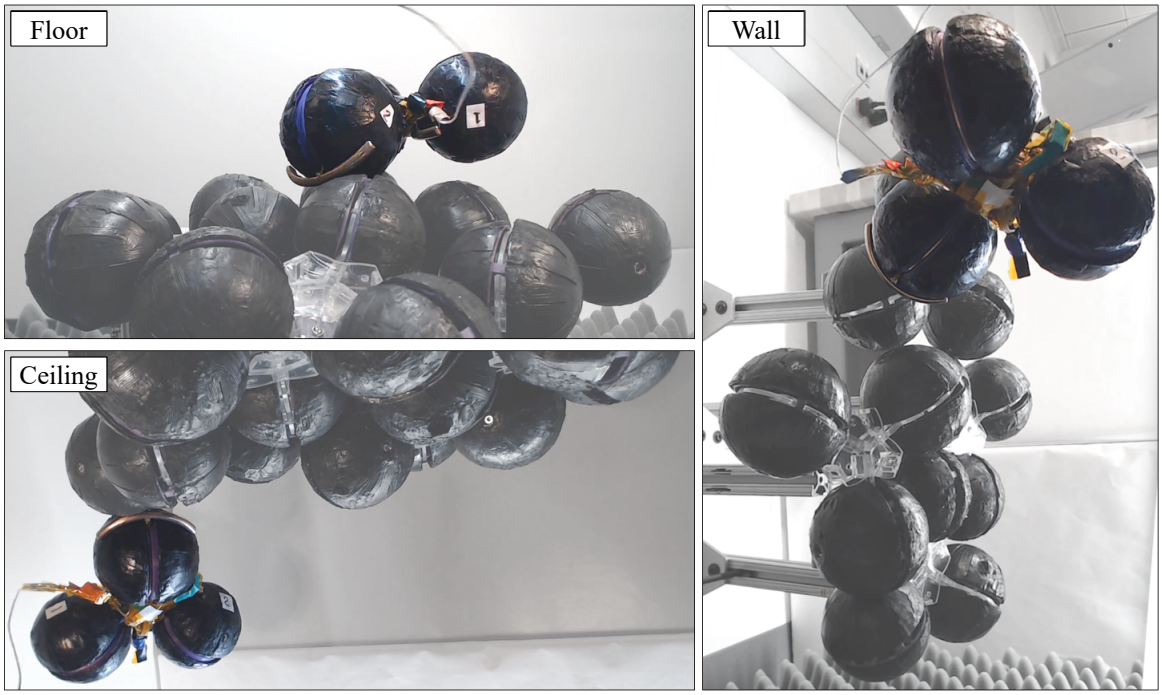

Fig. 10: The 3D continuous docks enabled FireAnt3D to successfully locomote on a floor, wall, and ceiling of its peers using a single style of locomotion.

Future work on a new FireAnt platform will focus on extending robot utility and practicality in three main ways. First, we will continue the development and refinement of the continuous dock by exploring the use of bespoke conductive plastics and will develop rapid and reliable manufacturing methods to mass-produce these docks. We will also perform full-factor experiments to further refine attachment parameters, as well as to statistically characterize the lifespan of the docks. Experiments will also be performed to evaluate dock performance in dirty, out-of-lab environments where traditional attachment mechanisms could jam.

Second, we will mature the design of FireAnt3D with a focus on reducing robot weight, part cost (currently about 500 USD), and complexity of assembly, as well as on increasing the speed of locomotion. We will also incorporate contact-based robot-to-robot communication as in [25] and [30]. These improvements will result in a scalable system, enabling the manufacture of a swarm of FireAnt robots able to execute self-assembling behaviors.

Finally, we will develop algorithms that enable future swarms of FireAnt robots to follow simple behaviors to self-assemble the sorts of non-latticed, environment-adaptive structures seen in nature, illustrated in Fig. 11. Because much of the existing literature only considers self-assembly in the context of prescribed, latticed shapes, new methods will need to be developed.

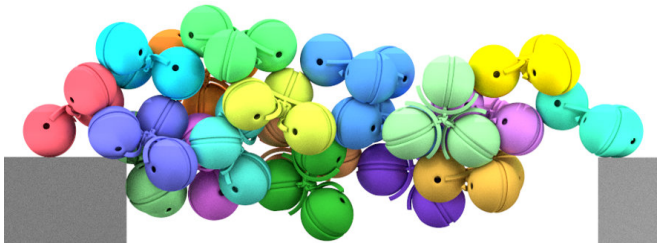

Fig. 11: Future swarms of FireAnt3D robots will build non-latticed structures, such as bridges that allow the swarm to cross large gaps.

FireAnt3D presents a profoundly different method of approaching the robotic self-assembly problem and addresses many longstanding issues in the field. Unlike most other self-assembling robotic platforms, FireAnt3D attaches to its peers at any point on their body, allowing connections to form even when the structure deflection and the tolerance stack inevitable in large swarms would defeat fixed-attachment-point robotic platforms. We hope that the work outlined in this paper provides the impetus towards and means by which to implement large-scale, non-latticed robotic self-assembly.

Design material for FireAnt3D, including robot code, electrical schematics, and CAD models are available at [34]. The video accompanying this paper shows the attachment process and locomotion in detail.

References

[1] C. R. Reid, M. J. Lutz, S. Powell, A. B. Kao, I. D. Couzin, and S. Garnier, "Army ants dynamically adjust living bridges in response to a cost–benefit trade-off," *Proceedings of the National Academy of Sciences*, vol. 112, no. 49, pp. 15 113–15 118, 2015.

[2] S. Phonekeo, N. Mlot, D. Monaenkova, D. L. Hu, and C. Tovey, "Fire ants perpetually rebuild sinking towers," *Royal Society open science*, vol. 4, no. 7, p. 170 475, 2017.

[3] O. Peleg, J. M. Peters, M. K. Salcedo, and L. Mahadevan, "Collective mechanical adaptation of honeybee swarms," *Nature Physics*, vol. 14, no. 12, pp. 1193–1198, 2018.

[4] C. Anderson, G. Theraulaz, and J.-L. Deneubourg, "Self-assemblages in insect societies," *Insectes sociaux*, vol. 49, no. 2, pp. 99–110, 2002.

[5] N. J. Mlot, C. A. Tovey, and D. L. Hu, "Fire ants self-assemble into waterproof rafts to survive floods," *Proceedings of the National Academy of Sciences*, vol. 108, no. 19, pp. 7669–7673, 2011.

[6] P. C. Foster, N. J. Mlot, A. Lin, and D. L. Hu, "Fire ants actively control spacing and orientation within self-assemblages," *Journal of Experimental Biology*, vol. 217, no. 12, pp. 2089–2100, 2014.

[7] B. M. Gumbiner, "Cell adhesion: The molecular basis of tissue architecture and morphogenesis," *Cell*, vol. 84, no. 3, pp. 345–357, 1996.

[8] M. W. Jorgensen, E. H. Ostergaard, and H. H. Lund, "Modular atron: Modules for a self-reconfigurable robot," in *2004 IEEE/RSJ International Conference on Intelligent Robots and Systems (IROS)(IEEE Cat. No. 04CH37566)*, Ieee, vol. 2, 2004, pp. 2068–2073.

[9] J. Neubert, A. P. Cantwell, S. Constantin, M. Kalontarov, D. Erickson, and H. Lipson, "A robotic module for stochastic fluidic assembly of 3d self-reconfiguring structures," in *2010 IEEE International Conference on Robotics and Automation*, IEEE, 2010, pp. 2479–2484.

[10] J. W. Romanishin, K. Gilpin, S. Claici, and D. Rus, "3d m-blocks: Self-reconfiguring robots capable of locomotion via pivoting in three dimensions," in *2015 IEEE International Conference on Robotics and Automation (ICRA)*, IEEE, 2015, pp. 1925–1932.

[11] M. Yim, W.-M. Shen, B. Salemi, D. Rus, M. Moll, H. Lipson, E. Klavins, and G. S. Chirikjian, "Modular self-reconfigurable robot systems [grand challenges of robotics]," *IEEE Robotics & Automation Magazine*, vol. 14, no. 1, pp. 43–52, 2007.

[12] J. Werfel, K. Petersen, and R. Nagpal, "Designing collective behavior in a termite-inspired robot construction team," *Science*, vol. 343, no. 6172, pp. 754–758, 2014.

[13] K. Gilpin, A. Knaian, and D. Rus, "Robot pebbles: One centimeter modules for programmable matter through self-disassembly," in *2010 IEEE International Conference on Robotics and Automation*, IEEE, 2010, pp. 2485–2492.

[14] J. Baca, S. Hossain, P. Dasgupta, C. A. Nelson, and A. Dutta, "Modred: Hardware design and reconfiguration planning for a high dexterity modular self-reconfigurable robot for extra-terrestrial exploration," *Robotics and Autonomous Systems*, vol. 62, no. 7, pp. 1002–1015, 2014.

[15] M. Rubenstein, K. Payne, P. Will, and W.-M. Shen, "Docking among independent and autonomous conro self-reconfigurable robots," in *IEEE International Conference on Robotics and Automation, 2004. Proceedings. ICRA'04. 2004*, IEEE, vol. 3, 2004, pp. 2877–2882.

[16] N. J. Wilson, S. Ceron, L. Horowitz, and K. Petersen, "Scalable and robust fabrication, operation, and control of compliant modular robots," *Frontiers in Robotics and AI*, vol. 7, p. 44, 2020.

[17] H. Kurokawa, K. Tomita, A. Kamimura, S. Kokaji, T. Hasuo, and S. Murata, "Distributed self-reconfiguration of m-tran iii modular robotic system," *The International Journal of Robotics Research*, vol. 27, no. 3-4, pp. 373–386, 2008.

[18] A. Spröwitz, R. Moeckel, M. Vespignani, S. Bonardi, and A. J. Ijspeert, "Roombots: A hardware perspective on 3d self-reconfiguration and locomotion with a homogeneous modular robot," *Robotics and Autonomous Systems*, vol. 62, no. 7, pp. 1016–1033, 2014.

[19] U. A. Fiaz and J. S. Shamma, "Usbot: A modular robotic testbed for programmable self-assembly," *IFAC-PapersOnLine*, vol. 52, no. 15, pp. 121–126, 2019.

[20] J. G. Bralla, *Design for manufacturability handbook*. McGraw-Hill, 1999.

[21] F. Scholz, "Tolerance stack analysis methods," *Research and technology boeing information & support services, boeing, seattle*, pp. 1–44, 1995.

[22] T. Tucci, B. Piranda, and J. Bourgeois, "A distributed self-assembly planning algorithm for modular robots," in *Proceedings of the 17th International Conference on Autonomous Agents and MultiAgent Systems*, International Foundation for Autonomous Agents and Multiagent Systems, 2018, pp. 550–558.

[23] K. Stoy and R. Nagpal, "Self-repair through scale independent self-reconfiguration," in *2004 IEEE/RSJ International Conference on Intelligent Robots and Systems (IROS)(IEEE Cat. No. 04CH37566)*, IEEE, vol. 2, 2004, pp. 2062–2067.

[24] N. Melenbrink, P. Michalatos, P. Kassabian, and J. Werfel, "Using local force measurements to guide construction by distributed climbing robots," in *2017 IEEE/RSJ International Conference on Intelligent Robots and Systems (IROS)*, IEEE, 2017, pp. 4333–4340.

[25] M. Malley, B. Haghighat, L. Houel, and R. Nagpal, "Eciton robotica: Design and algorithms for an adaptive self-assembling soft robot collective,"

[26] M. Shimizu and A. Ishiguro, "An amoeboid modular robot that exhibits real-time adaptive reconfiguration," in *2009 IEEE/RSJ International Conference on Intelligent Robots and Systems*, IEEE, 2009, pp. 1496–1501.

[27] S. Li, R. Batra, D. Brown, H.-D. Chang, N. Ranganathan, C. Hoberman, D. Rus, and H. Lipson, "Particle robotics based on statistical mechanics of loosely coupled components," *Nature*, vol. 567, no. 7748, pp. 361–365, 2019.

[28] F. Mondada, G. C. Pettinaro, A. Guignard, I. W. Kwee, D. Floreano, J.-L. Deneubourg, S. Nolfi, L. M. Gambardella, and M. Dorigo, "Swarm-bot: A new distributed robotic concept," *Autonomous robots*, vol. 17, no. 2-3, pp. 193–221, 2004.

[29] F. Wang, Z. Qian, Z. Yan, C. Yuan, and W. Zhang, "A novel resilient robot: Kinematic analysis and experimentation," *IEEE Access*, 2019.

[30] P. Swissler and M. Rubenstein, "Fireant: A modular robot with full-body continuous docks," in *2018 IEEE International Conference on Robotics and Automation (ICRA)*, IEEE, 2018, pp. 6812–6817.

[31] L. Cucu, M. Rubenstein, and R. Nagpal, "Towards self-assembled structures with mobile climbing robots," in *2015 IEEE International Conference on Robotics and Automation (ICRA)*, IEEE, 2015, pp. 1955–1961.

[32] T. Zhang, W. Zhang, and M. M. Gupta, "An underactuated self-reconfigurable robot and the reconfiguration evolution," *Mechanism and Machine Theory*, vol. 124, pp. 248–258, 2018.

[33] Proto-Pasta, *Conductive pla faq*, https://www.proto-pasta.com/pages/conductive-pla, Accessed: 2020-02-20.

[34] P. Swissler, *Github repository with fireant3d design material*, https://github.com/pswiss/Swissler-2020-FireAnt3D-Design.